Multi-wafer 3C–SiC heteroepitaxial growth on Si(100) substrates*

Sun Guo-Sheng(孙国胜)[a)b)†], Liu Xing-Fang(刘兴昉)[a)b)], Wang Lei(王 雷)[b)], Zhao Wan-Shun(赵万顺)[b)], Yang Ting(杨 挺)[b)], Wu Hai-Lei(吴海雷)[b)], Yan Guo-Guo(闫果果)[b)], Zhao Yong-Mei(赵永梅)[c)], Ning Jin(宁 瑾)[c)], Zeng Yi-Ping(曾一平)[a)b)], and Li Jin-Min(李晋闽)[a)b)]

[a)] *Key Laboratory of Semiconductor Materials Science, Institute of Semiconductors, Chinese Academy of Sciences, Beijing* 100083, *China*

[b)] *Material Science Center, Institute of Semiconductors, Chinese Academy of Sciences, Beijing* 100083, *China*

[c)] *State Key Laboratory of Transducer Technology, Chinese Academy of Sciences, Beijing* 100083, *China*

(Received 13 November 2009; revised manuscript received 22 December 2009)

Epitaxial growth of semiconductor films in multiple-wafer mode is under vigorous development in order to improve yield output to meet the industry increasing demands. Here we report on results of the heteroepitaxial growth of multi-wafer 3C–SiC films on Si(100) substrates by employing a home-made horizontal hot wall low pressure chemical vapour deposition (HWLPCVD) system which was designed to be have a high-throughput, multi-wafer (3×2-inch) capacity. 3C–SiC film properties of the intra-wafer and the wafer-to-wafer including crystalline morphologies, structures and electronics are characterized systematically. The undoped and the moderate NH_3 doped n-type 3C–SiC films with specular surface are grown in the HWLPCVD, thereafter uniformities of intra-wafer thickness and sheet resistance of the 3C–SiC films are obtained to be 6%∼7% and 6.7%∼8%, respectively, and within a run, the deviations of wafer-to-wafer thickness and sheet resistance are less than 1% and 0.8%, respectively.

Keywords: 3C–SiC, heteroepitaxial, multi-wafer, uniformity

PACC: 8115H, 6855

1. Introduction

Silicon carbide (e.g. 4H–SiC, 3C–SiC), owing to its unique characteristics such as high thermal stability, large band gap, resistance to chemical attack, and high critical breakdown electric field, now has become one of the state-of-art semiconductor materials for high-power, high temperature electronic devices[1−4] and micro-electromechanical system (MEMS) devices used in harsh environments.[5,6] SiC-based devices with superior operating characteristics[7] are under urgent demands, which will promote the developments of SiC substrates and SiC homo/heteroepitaxial films. As for SiC film growth, the traditional growth method was performed with the standard reactants of SiH_4 and either C_3H_8 or C_2H_4 in H_2 as the carrier gas,[8,9] by using a low pressure chemical vapour deposition (LPCVD) system in the manner of one wafer within a run. Therefore, multiple-wafer growth within a run is under vigorous development in order to improve yield output to meet the industry increasing demands.[10] To date, several groups have grown SiC films in multi-wafer mode either in commercial or home-made hot wall planetary LPCVD systems.[11−13] One of the most concerned issues is the uniformities of the intra-wafer and the wafer-to-wafer doping and growth rate in the multi-wafer system. When the growth chamber of the multi-wafer system is designed for accommodating increasing capacity, gas flow distribution and temperature distribution become more complicated than those of a traditional single-wafer system. We develop a home-made multi-wafer LPCVD by installing an inlet channel (IC) and an outlet channel (OC) in the LPCVD system. Compared with a single-wafer system, the multi-wafer system includes a large growth chamber (GC) where multiple wafers are mounted, an IC in the front (upstream side) and an OC in the rear (downstream side) of the GC as seen in Fig. 1. Gas

*Project supported by the National Natural Science Foundation of China (Grant Nos. 60876003 and 60606003) and the Science Foundation of the Chinese Academy of Sciences (Grant No. yz200702).

†Corresponding author. E-mail: gshsun@red.semi.ac.cn

© 2010 Chinese Physical Society and IOP Publishing Ltd

flow distribution is more controllable and uniform in such a configuration, thereby yielding highly uniform 3×5.08-cm SiC epilayers.

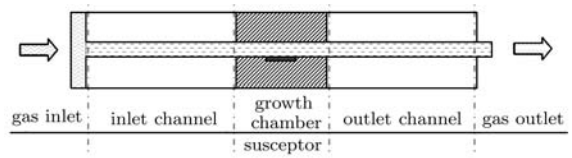


Fig. 1. Schematic illustration of the home-made multi-wafer HWLPCVD system.

2. Experiment

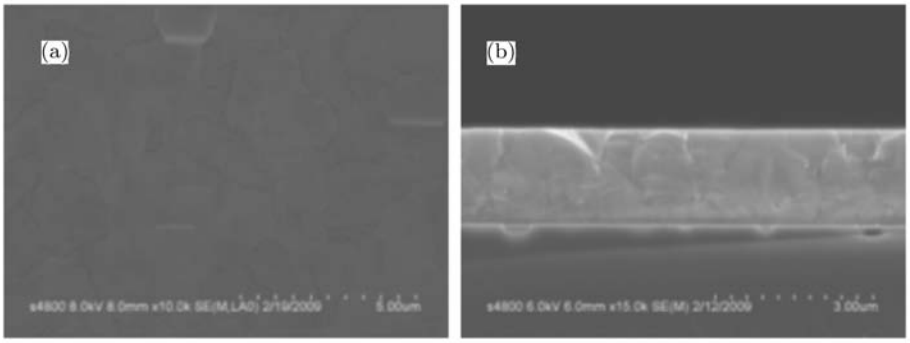
Multi-wafer 3C–SiC films have been heteroepitaxially grown on Si(100) substrates in a home-made HWLPCVD system, the schematic illustration of the HWLPCVD is shown Fig. 1. SiH_4 and C_2H_4 were used as silicon and carbon sources, respectively. The sources diluted and carried by pure H_2 gas were fed into the growth chamber through an inlet channel (as seen in Fig. 1). Before loaded into the growth chamber, Si(100) was washed with a conventional method and rinsed in HF diluted solution to remove the native oxidation from the surface. Further surface cleaning process was performed in the growth chamber with a H_2 atmosphere at 1000 °C for 30 min. The two-step growth method[14] was processed as follows: 1) carbonization. 5-sccm C_2H_4 diluted in 3-slm H_2 was used for carbonization and introduced into the growth chamber at 800 °C then the chamber temperature increased slowly with a rate of 50 °C min from 800 °C to 1050 °C. Carbonization was performed at 1050 °C for 20 min. 2) 3C–SiC heteroepitaxial growth. After carbonization, the chamber temperature was increased up to 1280 °C in 10 min, and then the silicon source SiH_4 was introduced. Heteroepitaxial growth was performed at 1280 °C with fluxes of H_2, SiH_4 and C_2H_4 being 3 slm, 1 sccm and 2 sccm, respectively. The growth chamber cooled down naturally at a H_2 atmosphere after heteroepitaxial growth. The pressure was kept at 2.6×10^4 Pa in the whole processing.

After growth, the films were characterized and analysed by scanning electron microscope (SEM), atomic force microscopy (AFM), x-ray diffraction (XRD) and sheet resistance measurement (SRM), separately. XRD was performed to analyse the film structures by using a Philips diffractometer with Cu–Kα radiation and θ–2θ geometry. SEM was used to study the surface morphology, by observing the cross-sectional shape and measuring the film thickness. AFM was employed to measure the surface morphology and root mean square (RMS), with a digital instruments multimode nanoscope IIIa operated in a contact mode. SRM was obtained by Napson NC-40 non-contact sheet resistance measurement instrument.

3. Results and discussion

The surfaces of SiC films were mirror-like and observed by optical microscope at low magnification. Figure 2 shows the surface morphological structures and the cross sectional morphological structures of the SiC films. The film thicknesses were about 1.7 μm. The 3C–SiC layers are mosaic in nature, and larger grain size provides evidence of better surface quality. The average grain size and the surface roughness were about 3 μm and 4.5 nm for an area of 10 μm×10 μm respectively (as seen in Fig. 2(c)). It has been reported that the SiC grains exposed at the surface had nearly the same size as the grains measured by AFM.[8] The size of the crystal grains followed a proportional relationship to growth rate and film thickness.[15]

When 3C–SiC film grew heteroepitaxially, nuclei grew two-dimensionally on the substrate surface and coalesced when the growing-up neighbour nuclei closely touched with each other, forming larger islands. Thereafter, the neighbour islands coalesced,



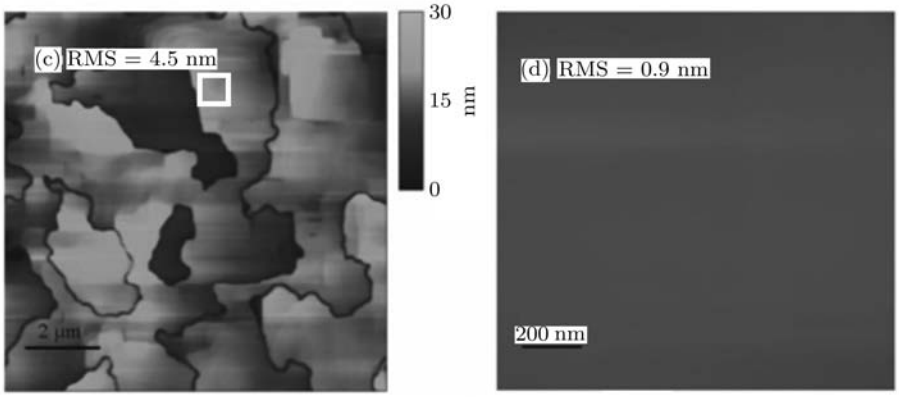


Fig. 2. Surface and cross-sectional SEM morphologies of 3C–SiC grown on Si(100). (a) Surface SEM morphology, (b) cross-sectional SEM morphology, film thickness is about 1.7 μm, (c) and (d) surface AFM morphologies, image sizes are 10 ×10 μm^2 and 1×1 μm^2, respectively. (d) Image zoomed in from the square area of (c) (quoted by the white frame).

leading to large platens of 3C–SiC formed on the surface. 3C–SiC platens were single crystal (as seen in Fig. 2(d)), however, the platen tilted with respect to each other, giving rise to different crystal domains which formed anti-phase domain (APD) boundaries (as seen in Figs. 2(a) and 2(c)). It has been demonstrated that aggressive etching processes may cause preferential etching at the boundaries of the APDs,[16,17] therefore, APDs would be decreased by an additional H_2 etching processing.[17]

Voids were detected at the interface between silicon substrate and the covered SiC film (as seen in Fig. 2(b)). The void was formed in the carbonization stage, when the Si substrate surface was not covered throughout by the first initial SiC carbonization layer, therefore, voids were formed at sites where surface Si atoms were intense out-diffusion at high temperatures. Out-diffusion of Si is effective at temperatures above 1100 °C and high-density voids are formed at lower growth temperatures (1100 °C–1150 °C).[18] Since the size and the density of the void are related to the growth parameter,[9] void free films will be obtained in an optimized growth processing.

Figure 3 shows the XRD spectra of three wafers within a run. The spectra are highly uniform, and peak position of each SiC(100) is almost the same, and the full-width at half-maximum (FWHM) is narrow, less than 0.5°. The peak position of SiC(100) at ∼41.3° corresponds to a lattice constant of 4.3622 Å (1 Å = 0.1 nm), which is slightly larger than that of single crystalline 3C–SiC (4.3596 Å). The spectra exhibits a strong SiC(100) texture without SiC(111) texture, therefore, SiC films show the orientation much the same as that of the Si(100) substrate, which indicates that the films are of homocrystalline cubic 3C–SiC. The growth rate is about 2 μm/h, and it should be noticed that if growth rate is higher than a certain value, SiC(111) texture will appear together with SiC(100) texture in the heteroepitaxial 3C–SiC films. Weak peak of SiC(222) texture at 75.5° appears, and it may be caused by the tilt SiC planes when islands coalesce, where the APD is formed as seen in Fig. 2(c). Peak at 69.15° arises, owing to the diffraction from Si(400) plane. The intensity of SiC(100) is much higher than that of Si(400), indicating a moderate 3C–SiC film thickness.

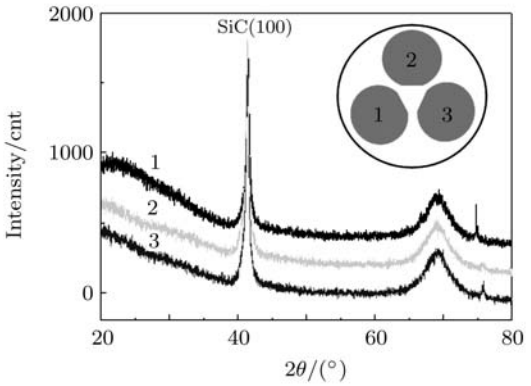


Fig. 3. The x-ray diffraction spectra of 3C–SiC films grown on Si(100) substrate. The (100) peak positions of wafers (No. 1, No. 2 and No. 3) are 41.45°, 41.37° and 41.35° respectively, and the corresponding FWHMs are 0.488°, 0.465° and 0.483° respectively.

Thickness and the sheet resistance uniformity are analysed by sampling three wafers within a run. Thickness measurement of each wafer is taken at eleven positions. Position 0 is located in the wafer centre. Five positions (labeled as 1∼5) are evenly distributed at a radius parallel to the primary plane, and the other five positions (labeled as –1∼–5) are evenly distributed at a radius perpendicular to the primary plane as seen in Fig. 4(a). Thickness uniformity of each wafer is calculated by the following equation:

$$\sigma/M = \sum_{i=1}^{N} \left(t_i - \left(\sum_{i=1}^{N} t_i \right) \Big/ N \right)^2 \Big/ \sum_{i=1}^{N} t_i \times 100\%, \tag{1}$$

where t_i is the thickness of the i-th position, N is the total sample counts. For the films with a thickness of about 5 μm, the σ/M values of intra-wafer and wafer-to-wafer are about 6%∼7% and less than 1%, respectively, which indicates that good thickness uniformity is achieved in the 3C–SiC heteroepitaxial thin films.

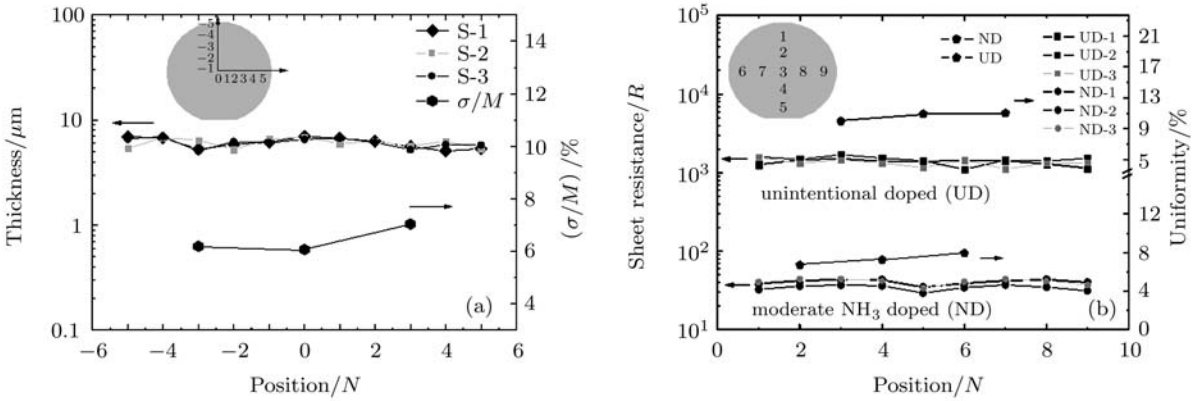


Fig. 4. Thickness and sheet resistance uniformities of 3C–SiC films grown on Si(100) substrates. (a) Thickness and uniformities (σ/M) of 3C–SiC samples S-1, S-2 and S-3, respectively, within a run, (b) sheet resistances and uniformities of UD and ND 3C–SiC samples. Lines are guides to the eye.

Sheet resistance measurement of each wafer is taken at nine positions as seen in Fig. 4(b). Position 3 is located in the wafer centre. The other eight positions are evenly distributed at two diameters mutually perpendicular to each other. Sheet resistance, which presents the resistance in the current direction of a square-shaped thin film, can be expressed as $R_{\rm K} = \rho/d$, where ρ is the film resistivity, and d is the film thickness. Sheet resistance ($R_{\rm K}$) uniformity can be used to represent doping uniformity of 3C–SiC heteroepitaxial thin films. Figure 4(b) shows $R_{\rm K}$ and uniformities of undoped (UD) and moderate NH_3 doped (ND) n-type 3C–SiC thin films, respectively. For UD films, $R_{\rm K}$ is at a magnitude of 10^3 $\Omega/\Box$, the uniformities of intra-wafer and wafer-to-wafer are about 9%∼10.5% and less than 0.8%, respectively. For ND films, $R_{\rm K}$ is at magnitude of 10^1 $\Omega/\Box$, the uniformities of intra-wafer and wafer-to-wafer are about 6.7%∼8% and less than 1.2%, respectively. Compared with the UD films, the ND films have good intrawafer uniformity but degrade wafer-to-wafer uniformity. However, the difference in uniformity between ND and UD films was trivial on the whole.

4. Conclusion

Multi-wafer (3×2-inch) 3C–SiC heteroepitaxial films are grown on Si(100) substrates by using a home-made horizontal hot wall low pressure chemical vapour deposition (HWLPCVD) system. Undoped and moderate NH_3 doped n-type 3C–SiC films with mirror-like surface are obtained. 3C–SiC film properties, including crystalline morphologies, structures and electronics, are characterized and analysed in the way of intra-wafer and wafer-to-wafer. The uniformities of intra-wafer thickness and sheet resistance of the 3C–SiC films are obtained to be 6%∼7% and 6.7%∼8%, respectively, within a run, and the deviations of wafer-to-wafer thickness and sheet resistance are less than 1% and 0.8%, respectively. It is indicated that good uniformity has been achieved in the 3C–SiC heteroepitaxial thin films.

References

[1] Zhang Y R, Zhang B, Li Z J, Deng X C and Liu X L 2009 *Chin. Phys.* B **18** 3995

[2] Kumar M J and Rao D V 2004 *IEEE Proceedings-Circ. Dev. Syst.* **151** 63

[3] Rahimi R, Miller C M, Munger A, Raghavan S, Stinespring C D and Korakakis D 2009 *Mater. Res. Soc. Symp. Proceedings* **1129** 67

[4] Patil A, Fu X A, Neudeck P, Beheim G, Mehregany M and Garverick S 2009 *Materials Science Forum* **600–603** 1083

[5] Mehregany M, Zorman C A, Rajan N and Wu C H 1998 *Proceedings of the IEEE* **86** 1594

[6] Locke C, Kravchenko G, Waters P, Reddy J D, Du K, Volinsky A A, Frewin C L and Saddow S E 2009 *Materials Science Forum* **615–617** 633

[7] Davis R F, Kelner G, Shur M, Palmour J W and Edmond J A 1991 *Proceedings of the IEEE* **79** 677

[8] Roper C S, Radmilovic V, Howe R T and Maboudian R 2008 *J. Appl. Phys.* **103** 084907

[9] Scholz R, Gosele U, Niemann E, Leidich D and Wischmeyer F 1997 *Diam. Relat. Mater.* **6** 1365

[10] Burk A A, O'Loughlin M J, Sumakeris J J, Hallin C, Berkman E, Balakrishna V, Young J, Garrett L, Irvine K G and Powell A R 2009 *Materials Science Forum* **600–603** 77

[11] Burk A A, O'Loughlin M J and Mani S S 1998 *Silicon Carbide, III–Nitrides and Related Materials* Parts 1 and 2 **264–2** 83

[12] O'Loughlin M J, Nordby H D and Burk A A 1999 *Wide-Bandgap Semiconductors for High-Power, High-Frequency and High-Temperature Applications-1999* **572** 161

[13] Hecht C, Thomas B, Stein R and Friedrichs P 2009 *Materials Science Forum* **600–603** 95

[14] Nishino S, Powell J A and Will H A 1983 *Appl. Phys. Lett.* **42** 460

[15] Saddow S E, Okhusyen M E, Mazzola M S, Dudley M, Huang X R, Huang W, Su H, Shamsuzzoha M and Lo Y H 1999 *III–V and IV–IV Materials and Processing Challenges for Highly Integrated Microelectronics and Optoelectronics* **535** 107

[16] Coletti C, Hetzel M, Virojanadara C, Starke U and Saddow S E 2006 *Silicon Carbide 2006—Materials, Processing and Devices* **911** 131

[17] Coletti C, Frewin C L, Saddow S E, Hetzel M, Virojanadara C and Starke U 2007 *Appl. Phys. Lett.* **91** 061914

[18] Gupta A, Sengupta J and Jacob C 2008 *Thin Solid Films* **516** 1669